Evidence for the Importance of Extended Coulomb Interactions and Forward Scattering in Cuprate Superconductors

S. Johnston,[1,4] I. M. Vishik,[1,2,3] W. S. Lee,[1,2] F. Schmitt,[1,2] S. Uchida,[5] K. Fujita,[6] S. Ishida,[5] N. Nagaosa,[7,8] Z. X. Shen,[1,2,3] and T. P. Devereaux[1,2]

[1]*Stanford Institute for Materials and Energy Sciences, SLAC National Accelerator Laboratory and Stanford University, Menlo Park, California 94305, USA*
[2]*Geballe Laboratory for Advanced Materials, Stanford University, Stanford, California 94305, USA*
[3]*Department of Physics and Applied Physics, Stanford University, Stanford, California 94305, USA*
[4]*IFW Dresden, P.O. Box 27 01 16, D-01171 Dresden, Germany*
[5]*Department of Physics, Graduate School of Science, University of Tokyo, Bunkyo-Ku, Tokyo 113-0033, Japan*
[6]*Laboratory for Atomic and Solid State Physics, Department of Physics, Cornell University, Ithaca, New York 14853, USA*
[7]*Department of Applied Physics, University of Tokyo, Bunkyo-ku, Tokyo 113-8656, Japan*
[8]*Cross-Correlated Materials Research Group (CMRG) and Correlated Electron Research Group (CERG), RIKEN-ASI, Wako 351-0198, Japan*

(Received 6 January 2011; revised manuscript received 13 December 2011; published 20 April 2012)

The prevalent view of the high-temperature superconducting cuprates is that their essential low-energy physics is captured by local Coulomb interactions. However, this view been challenged recently by studies indicating the importance of longer-range components. Motivated by this, we demonstrate the importance of these components by examining the electron-phonon (e-ph) interaction with acoustic phonons in connection with the recently discovered renormalization in the near-nodal low-energy ($\sim$ 8–15 meV) dispersion of $Bi_2Sr_2CaCu_2O_{8+\delta}$. By studying its nontrivial momentum and doping dependence we conclude a predominance of forward scattering arising from the direct interplay between the e-ph and extended Coulomb interactions. Our results thus demonstrate how the low-energy renormalization can provide a pathway to new insights into how these interactions interplay with one another and influence pairing and dynamics in the cuprates.

DOI: 10.1103/PhysRevLett.108.166404 PACS numbers: 71.38.−k, 74.72.−h, 74.25.Jb

As in all transition metal oxides, strong correlations play an important role in the cuprates. The cuprates are on the verge of localization (or delocalization) and/or ionicity (or covalency) that can be tuned with doping of either holes or electrons. This is most apparent in the Coulomb interaction of these systems where metallic screening exhibited by the overdoped cuprates is lost as the insulating phase is approached at half filling. Understanding the role of the nonlocal components of the Coulomb interaction (beyond the canonical on-site Hubbard interaction) in this process is important. Their inclusion can suppress correlation-induced contributions to d-wave pairing [1], promote phase separation [2], and produce nontrivial renormalizations of the electron-phonon (e-ph) interactions [3,4].

The loss of metallicity with underdoping also produces anomalous screening of the e-ph interactions. Here we examine this idea in the context of coupling to the in-plane polarized acoustic phonon branch as the origin of the recently discovered renormalization in the near-nodal low-energy ($\sim$ 8–15 meV) dispersion of $Bi_2Sr_2CaCu_2O_{8+\delta}$ (Bi-2212) [5–9] (Fig. 1). We show that the involvement of long-range components of the screened Coulomb interaction resolves the puzzle of how a mode-coupling feature observed in angle-resolved photoemission spectroscopy (ARPES) can appear below the maximum superconducting gap energy. This result indicates that the combined interplay between the e-ph interaction, the extended Coulomb interaction, and the breakdown of metallic screening with underdoping are crucial for understanding not only the energy scale of this renormalization but also its momentum and doping dependence. The strong doping dependence inferred in this study also provides new insights into the discrepancy between the strength of the e-ph interaction predicted by density functional theory (DFT) [10] and those inferred experimentally [11,12], as well as the evolution to strong e-ph coupling in undoped systems observed in optical [13] and ARPES studies [14,15].

In Fig. 1(a) we present raw ARPES spectra along the nodal $(0, 0) - (\pi, \pi)$ direction of underdoped Bi-2212 ($T_c = 55$ K, hole-doped $p \sim 0.08$, UD55K) and the corresponding momentum distribution curve (MDC) analysis [Figs. 1(b) and 1(c)]. The experimental setup is identical to that of Ref. [6] with an energy resolution of 3 meV. Both the well-known 70 meV [12,16] and low-energy band renormalizations [5–9] are apparent in the raw data [Fig. 1(b), indicated by arrows]. Focusing on the latter, the low-energy renormalization manifests as a subtle bend in the dispersion with an accompanying change in spectral weight at an energy $\sim$8–15 meV. This energy scale interestingly appears below the maximum of the superconducting gap Δ_0,

 © 2012 American Physical Society

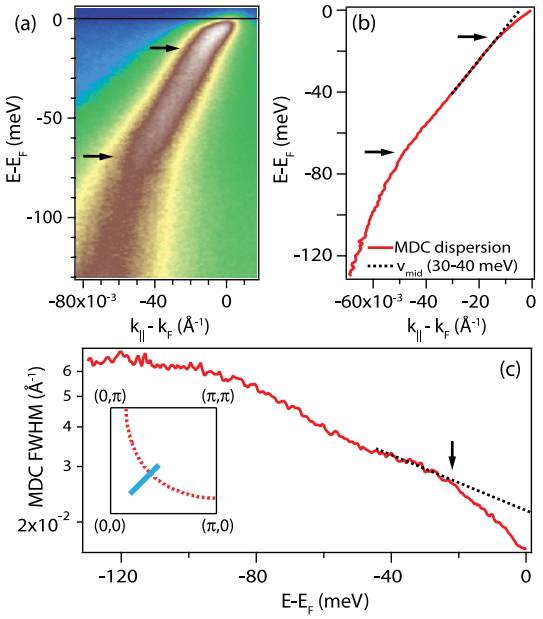

FIG. 1 (color online). Nodal low-energy dispersion renormalization in Bi-2212 UD55 (11 K). (a) Color image plot of the raw data with both the low-energy and 70 meV renormalizations marked by arrows. (b) The band dispersion derived by fitting the momentum distribution curves (MDC) at each energy in (a) with a Lorentzian line shape. The low-energy renormalization is defined by the deviation of the dispersion from v_{mid}, the velocity fit between 30–40 meV (dotted line). (c) The MDC FWHM which shows a more rapid decrease close to E_F as a consequence of the renormalization of the low-energy dispersion.

which implies a strong momentum dependence for the e-ph vertex $g(\mathbf{k}, \mathbf{q})$ for quasiparticle scattering from momentum state $|\mathbf{k}\rangle$ to $|\mathbf{k} + \mathbf{q}\rangle$. This conclusion stems from the contrast with the case of coupling to a sharp bosonic mode with a weakly momentum-dependent $g(\mathbf{k}, \mathbf{q})$, where the electronic dispersion is renormalized at an energy $\Omega + \Delta_0$ set by the mode energy Ω shifted by Δ_0 [17]. This shift occurs for *all* quasiparticles coupled to the mode, even those at the node where $\Delta(\mathbf{k})$ is zero, as the electron self-energy $\Sigma(\mathbf{k}, \omega)$ is given by a sum over all phonon scattering processes with momentum transfers $\mathbf{q}$ spanning the Brillouin zone. Therefore, when $g(\mathbf{k}, \mathbf{q})$ is relatively momentum independent, all scattering processes are comparably weighted and $\Sigma(\mathbf{k}, \omega)$ dominated by contributions from the large number of final states at the gap edge Δ_0 in the superconducting state. However, if $g(\mathbf{k}, \mathbf{q})$ is sufficiently peaked as to weight out these same final states then features can be produced in the dispersion below Δ_0 [18]. In the case of nodal electrons, $g(\mathbf{k}, \mathbf{q})$ must be peaked in the forward scattering direction (small $\mathbf{q}$) so as to weight out large $\mathbf{q}$ scattering to the antinodal region. Such is the case for the in-plane acoustic branch in the cuprates, as elaborated below.

A first-order coupling between the electrons and acoustic phonons arises via the modulation of the screened Coulomb potential [19]. Here, the displacements of the ions from their equilibrium position induce quasiparticle scattering while the involvement of the screened Coulomb potential results in the forward scattering peak in the coupling as metallicity breaks down. In this case the e-ph vertex reduces to a function of momentum transfer only with $g(\mathbf{q}) = V_{\mathrm{cell}}^{-1}\sqrt{\hbar/2M\Omega(\mathbf{q})}\hat{e}_{\mathbf{q}} \cdot \mathbf{q}V(\mathbf{q})/\epsilon(\mathbf{q})$ where $\hat{e}_{\mathbf{q}}$ and $\Omega(\mathbf{q})$ are the polarization and dispersion of the acoustic branch, respectively, M is the sum of the Cu and O mass, $V(\mathbf{q}) = 4\pi e^2/\epsilon q^2$ is the bare Coulomb potential, ϵ is the static dielectric constant, and $\epsilon(\mathbf{q})$ is the momentum-dependent dielectric function. To model the effects of screening we assume a simple Thomas-Fermi form $\epsilon(\mathbf{q}) = (1 + q_{\mathrm{TF}}^2/q^2)$, where q_{TF} is the Thomas-Fermi wave vector. This leads to an overall momentum dependence [apart from the phonon dispersion $\Omega(\mathbf{q})$] $g(\mathbf{q}) \propto \hat{e}_{\mathbf{q}} \cdot \mathbf{q}/(q^2 + q_{\mathrm{TF}}^2)$ which is peaked for $q \sim q_{\mathrm{TF}}$, vanishing for $\mathbf{q} \to 0$, and small for large $\mathbf{q}$. In this case contributions to the e-ph interaction occur from both the e-ph and Coulomb interactions via the magnitude of the momentum dependence of the dielectric function. In the cuprates metallic screening begins to break down with underdoping resulting in a small q_{TF} and subsequently $|g(\mathbf{q})|^2$ develops a pronounced peak at small $\mathbf{q}$ [20]. As a result, the nodal self-energy $\Sigma(\mathbf{k}, \omega)$ is determined from scattering to nearby states with a small superconducting gap and a peak is produced in $\Sigma(\mathbf{k})$ at an energy set by a weighted average of $<\Omega(\mathbf{q}) + \Delta(\mathbf{k})>_{g(\mathbf{q})} \leq \Delta_0$.

In order to demonstrate this more concretely we now compare calculated spectral functions $A(\mathbf{k}, \omega)$ directly to ARPES experiments. Here, $A(\mathbf{k}, \omega)$ is calculated using standard Migdal-Eliashberg theory [17,21]. [For details see the supplementary online material (SOM) [22].] The model includes coupling to the acoustic phonon branch ($q_{\mathrm{TF}} = 0.5/a$) and a spectrum of higher energy optical oxygen vibrations [20,23]. The acoustic dispersion is taken to be $\Omega(\mathbf{q}) = \Omega_0\sqrt{\sin^2(q_x a/2) + \sin^2(q_y a/2)}/\sqrt{2}$ and the top of the branch is set by $\Omega_0 = 15$ meV (the precise choice of Ω_0 is not critical to our conclusions, see SOM [22]). The superconducting gap is modeled with the usual d-wave form $\Delta(\mathbf{k}) = \Delta_0[\cos(k_x a) - \cos(k_y a)]/2$ with $\Delta_0 = 37$ meV. The lattice constants are $a = b = 3.8$ and $c = 7.65$ Å [24]. We take $\epsilon = 30\epsilon_0$, similar to the value in LSCO [25,26]. Finally, the bare band dispersion is taken from the parameterization of Ref. [27].

The calculated $A(\mathbf{k}, \omega)$ and MDC analysis applied to the simulated data are shown in Figs. 2(a)–2(c). Excellent agreement with experiment is obtained and the low-energy renormalization is reproduced at the correct energy scale in the raw spectral function [Fig. 2(a)] as well as the MDC-derived dispersion [Fig. 2(b)] and linewidths [Fig. 2(c)]. The strength of the coupling $\lambda(\mathbf{k})$, estimated from the ratio of the simulated Fermi velocities with (v_f) and without (v_f^0) coupling to the acoustic branch, $1 + \lambda = v_f^0/v_f$,

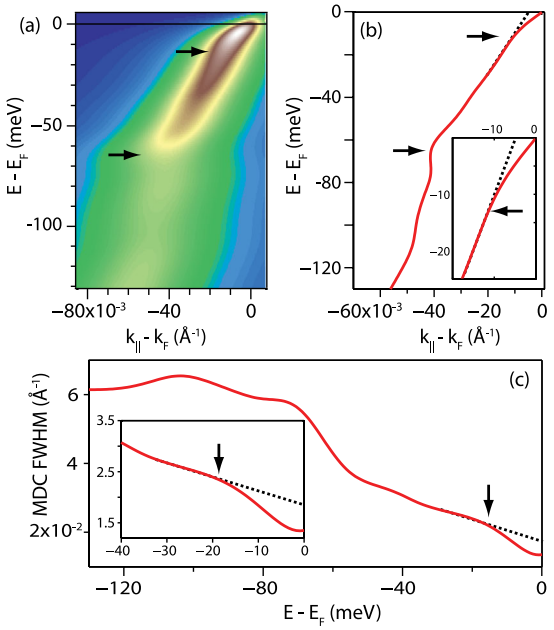

FIG. 2 (color online). (a) Calculated $A(\mathbf{k}, \omega)$ along the nodal direction $(0, 0)$–(π, π) in the superconducting state (25 K). Here, an additional component $\propto \omega^2$ has been added to the imaginary part of the self-energy to simulate broadening due to e-e interactions. (b) The MDC-derived dispersion and (c) MDC FWHM obtained from (a). The parameters used in the calculation are given in the text.

yields $\lambda(\mathbf{k}_{\text{node}}) = 0.67$, consistent with the observed magnitude of the renormalization [6,9].

In Figs. 3(a) and 3(b) we present experimental and calculated MDC-derived dispersions for a series of off-nodal cuts taken up to 11 degrees from the node. The data for underdoped Bi-2212 is presented here for the first time and covers a wider momentum range than previously examined [8]. Because of the improved resolution of this study no deconvolution methods have been applied to the data. Unless otherwise stated, the superconducting gap is determined independently for each cut by fitting symmetrized energy distribution curves at k_F to a minimal model [28] while the energy scale of the renormalization is determined from fitting the dispersion slope between 30–40 meV (v_{mid}), or by subtracting a linear band. As cuts are taken further from the node both the measured and calculated data show a shift in the gap and renormalization energies. This can be further quantified by using a linear band subtraction as shown in Figs. 3(d) and 3(e). The momentum dependence of the gap and renormalization energies are summarized in Fig. 3(f). The energy scale of the renormalization shifts for off-nodal cuts, following the local value of $\Delta(\mathbf{k})$ as shown here and in agreement with observations at optimal doping [8].

In Fig. 4 we present considerations for the doping dependence of the renormalization, which naturally emerges from the doping-driven changes in metallicity. To mimic this we vary q_{TF} and examine changes in the low-energy renormalization. The results are shown in Fig. 4(a) and the corresponding coupling strengths are shown in Fig. 4(b) where they are compared against estimates derived from previous ARPES studies [6,9]. For decreasing q_{TF} (underdoping) the coupling strength increases producing a stronger renormalization in agreement with experiment and implying a strongly doping-dependent interaction. This result should also survive the inclusion of the short-range Hubbard interaction, which further enhances the e-ph vertex at small $\mathbf{q}$ [29–31].

Our results show that the e-ph and Coulomb interactions have a strong interplay which produces a highly momentum- and doping-dependent coupling to the acoustic phonon branch. This has a number of important implications. The e-ph interaction is generally thought to play a secondary role in the high-T_c cuprates, a view supported by DFT studies predicting weak e-ph interactions in these systems [10,11]. In contrast, experimental estimates typically infer coupling strengths greater than those predicted and with a strong doping dependence. For example, in the doped systems, dispersion renormalizations [12,16,32] are observed which have been (controversially) interpreted as due to coupling to oxygen phonons [12] and which are well described by conventional theory. Conversely, in the undoped cuprates, polaronic effects are observed that demonstrably alter the spectral function from a Lorentzian to Gaussian line shape [14,15], requiring a strong coupling framework [4]. Such a framework also has been invoked to account for the position and structure of the midinfrared peak in the optical conductivity of the undoped cuprates [13]. These observations point to a strongly doping-dependent variation in the strength of the e-ph interaction as inferred here. Since this dependence is rooted in an interplay with the Coulomb interaction, it is not captured by DFT and helps to explain the discrepancy between the coupling strengths predicted by DFT [10] and those inferred from experiment [11,12,14,15].

The momentum dependence of the acoustic coupling effectively removes it from transport measurements, which are dominated by backscattering processes heavily weighted out by the forward scattering peak [29]. This peak is also expected to enhance superconductivity, as phonons with pronounced small $\mathbf{q}$ coupling are beneficial to d-wave pairing when acting in conjunction with an electronic mechanism [33]. Coupling to the acoustic branch can therefore enhance pairing in a multichannel scenario, adding to the attractive contribution mediated by c-axis optical oxygen modes and countering the repulsive contribution of the in-plane bond-stretching modes [20,33,34] (see SOM [22]). As such, a significant phonon-mediated contribution to pairing can be present that is hidden from bulk transport probes. However, anomalies in the linewidth

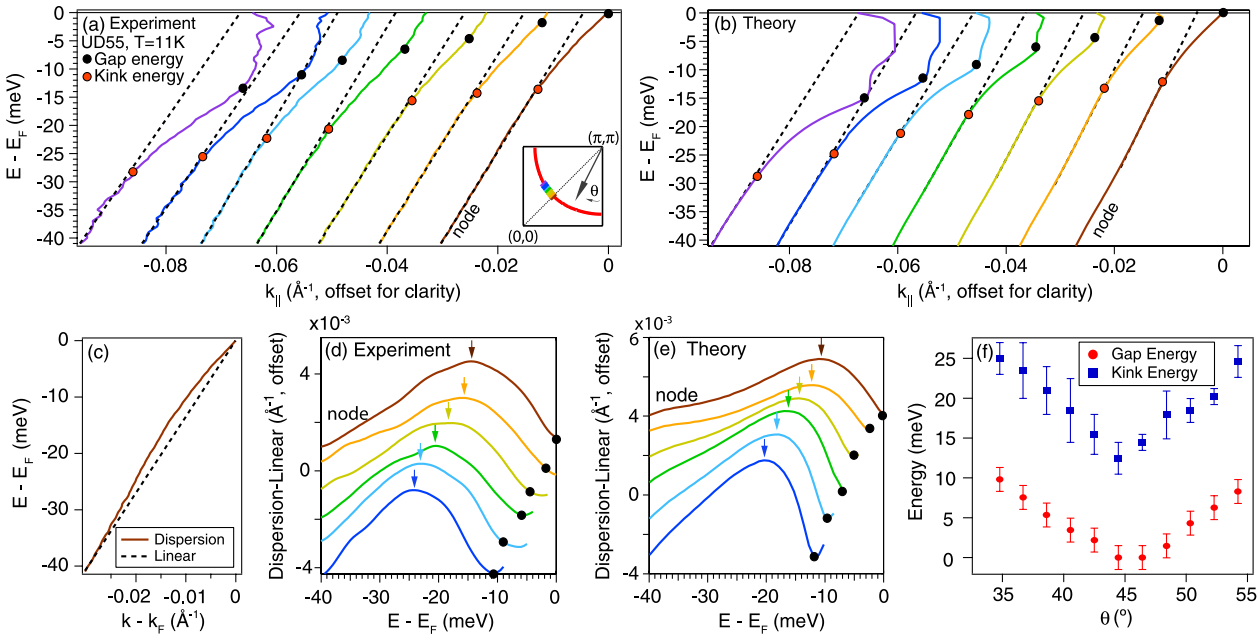

FIG. 3 (color online). Low-energy dispersion renormalization away from the node (theory/experiment UD55, $T = 11$ K). (a) MDC dispersions at the node (rightmost) and away from the node, offset horizontally for clarity. The black circles indicate the gap energy, determined by fitting symmetrized data to a minimal model [28]. The red circles indicate the approximate scale of the low-energy renormalization, determined from the deviation from v_{mid}. (b) MDC dispersions obtained from the calculated $A(\mathbf{k}, \omega)$. The parameters used here are identical to those used in Fig. 2. (c) A sketch of how the energy of the renormalization can be further quantified by subtracting a linear offset from the dispersion (shown here for a nodal cut) between the gap energy and 40 meV. (d) Difference in $\mathbf{k}$ between the dispersion and dotted line in (c) for cuts taken at the node (top) and progressively away from the node (towards the bottom). The data has been smoothed over 20 iterations and the curves are offset vertically for clarity. (e) As in (d) but obtained from the calculated $A(\mathbf{k}, \omega)$. (f) The momentum dependence of the gap and renormalization energies (from experiment), the latter determined by the method in (c). The error bars on the gap (1.5 meV), reflect uncertainty in determining E_F (0.5 meV) and uncertainty in the fit (0.5 meV) plus a 50% margin. Error bars for the renormalization energy reflect variation upon smoothing by different numbers of iterations.

of the acoustic phonon should appear for $q \sim q_{\mathrm{TF}}$ which may be detectable by x-ray scattering [35].

To summarize, we have examined the interplay between the e-ph and extended Coulomb interactions in the high-T_c cuprates and demonstrated a strong interplay between the two. For coupling to acoustic phonons, this interplay results in a renormalized e-ph interaction with a strong doping and momentum-dependence, peaked in the forward scattering direction. This coupling produces electronic renormalizations whose energy scale, doping, and momentum dependence are in excellent agreement with the recently discovered low-energy, near-nodal dispersion renormalization in Bi-2212. Our results indicate that the e-ph and extended Coulomb interactions are strongly intertwined, which plays an important role in establishing the low-energy electronic structure and physics of the cuprates. Therefore, we conclude the need to consider both interactions in order to obtain a complete picture of the high-T_c cuprates.

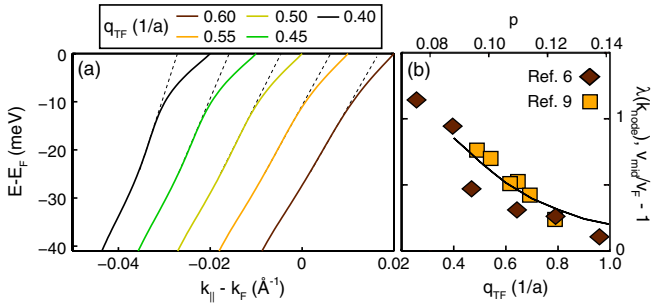

FIG. 4 (color online). (a) Nodal MDC-derived dispersions obtained from the model $A(\mathbf{k}, \omega)$ for different q_{TF}. (Any doping dependence of ϵ has been neglected.) (b) Solid line: $\lambda(\mathbf{k}_{\mathrm{node}})$ for the acoustic mode as a function of q_{TF}. Symbols: experimental estimates for $\lambda(\mathbf{k}_{\mathrm{node}}) = v_{\mathrm{mid}}/v_F - 1$ as a function of doping (Refs. [6,9]).

The authors thank B. Moritz, R. He, E. van Heumen, N. C. Plumb and D. Dessau for useful discussions. This work is supported by the DOE Office of Basic Energy Sciences, Division of Materials Sciences. S. J. acknowledges support from NSERC (Canada) and the Foundation for Fundamental Research on Matter (Netherlands).

Note added.—Recently, an anomalous broadening of the longitudinal acoustic phonon was reported in Bi-2201 at small $\mathbf{q}$ [35].

[1] A. S. Alexandrov and V. V. Kabanov, Phys. Rev. Lett. **106**, 136403 (2011).
[2] E. Dagotto, J. Riera, Y. C. Chen, A. Moreo, A. Nazarenko, F. Alcaraz, and F. Ortolani, Phys. Rev. B **49**, 3548 (1994).
[3] O. Rösch and O. Gunnarsson, Phys. Rev. Lett. **92**, 146403 (2004).
[4] A. S. Mishchenko and N. Nagaosa, Phys. Rev. Lett. **93**, 036402 (2004).
[5] N. C. Plumb, T. J. Reber, J. D. Koralek, Z. Sun, J. F. Douglas, Y. Aiura, K. Oka, H. Eisaki, and D. S. Dessau, Phys. Rev. Lett. **105**, 046402 (2010).
[6] I. Vishik *et al.*, Phys. Rev. Lett. **104**, 207002 (2010).
[7] W. Zhang *et al.*, Phys. Rev. Lett. **100**, 107002 (2008).
[8] J. D. Rameau, H.-B. Yang, G. D. Gu, and P. D. Johnson, Phys. Rev. B **80**, 184513 (2009).
[9] H. Anzai *et al.*, Phys. Rev. Lett. **105**, 227002 (2010).
[10] F. Giustino, M. L. Cohen, and S. G. Louie, Nature (London) **452**, 975 (2008).
[11] D. Reznik, G. Sangiovanni, O. Gunnarsson, and T. P. Devereaux, Nature (London) **455**, E6 (2008).
[12] A. Lanzara *et al.*, Nature (London) **412**, 510 (2001).
[13] A. S. Mishchenko, N. Nagaosa, Z.-X. Shen, G. De Filippis, V. Cataudella, T. P. Devereaux, C. Bernhard, K. W. Kim, and J. Zaanen, Phys. Rev. Lett. **100**, 166401 (2008).
[14] F. Ronning, K. M. Shen, N. P. Armitage, A. Damascelli, D. H. Lu, Z.-X. Shen, L. L. Miller, and C. Kim, Phys. Rev. B **71**, 094518 (2005).
[15] K. M. Shen *et al.*, Phys. Rev. B **75**, 075115 (2007).
[16] P. D. Johnson *et al.*, Phys. Rev. Lett. **87**, 177007 (2001).
[17] A. W. Sandvik, D. J. Scalapino, and N. E. Bickers, Phys. Rev. B **69**, 094523 (2004).
[18] E. G. Maksimov, O. V. Dolgov, and M. L. Kulić, Phys. Rev. B **72**, 212505 (2005).
[19] G. D. Mahan, in *Many-Particle Physics* (Plenum Press, New York), 2nd ed.
[20] S. Johnston, F. Vernay, B. Moritz, Z.-X. Shen, N. Nagaosa, J. Zaanen, and T. P. Devereaux, Phys. Rev. B **82**, 064513 (2010).
[21] W. S. Lee, S. Johnston, T. P. Devereaux, and Z.-X. Shen, Phys. Rev. B **75**, 195116 (2007).
[22] See Supplmental Material at http://link.aps.org/supplemental/10.1103/PhysRevLett.108.166404 for details.
[23] Since we focus on the low-energy renormalization the coupling to the optical modes is momentum independent with overall strengths $\lambda = 0.23$, 0.05 and 0.05 for the 36, 55, and 70 meV modes, respectively [20].
[24] N. N. Kovaleva *et al.*, Phys. Rev. B **69**, 054511 (2004).
[25] A. S. Alexandrov and A. M. Bratkovsky, Phys. Rev. Lett. **84**, 2043 (2000).
[26] D. N. Aristov and G. Khaliullin, Phys. Rev. B **74**, 045124 (2006).
[27] M. Eschrig and M. R. Norman, Phys. Rev. Lett. **85**, 3261 (2000). We apply a chemical potential to obtain $\langle n \rangle = 0.9$, followed by an overall renormalization of the bandwidth $Z = 0.9$ to reflect an underdoped system.
[28] M. R. Norman, M. Randeria, H. Ding, and J. C. Campuzano, Phys. Rev. B **57**, R11 093 (1998).
[29] M. L. Kulić and R. Zeyher, Phys. Rev. B **49**, 4395 (1994).
[30] Z. B. Huang, W. Hanke, and E. Arrigoni, and D. J. Scalapino , Phys. Rev. B **68**, 220507(R) (2003).
[31] R. Zeyher and M. L. Kulić, Phys. Rev. B **53**, 2850 (1996).
[32] T. Dahm, V. Hinkov, S. V. Borisenko, A. A. Kordyuk, V. B. Zabolotnyy, J. Fink, B. Büchner, D. J. Scalapino, W. Hanke, and B. Keimer, Nature Phys. **5**, 217 (2009).
[33] N. Bulut and D. J. Scalapino, Phys. Rev. B **54**, 14 971 (1996).
[34] A. Nazarenko and E. Dagotto, Phys. Rev. B **53**, R2987 (1996).
[35] C. J. Bonnoit, D. R. Gardner, R. Chisnell, A. H. Said, Y. Okada, T. Kondo, T. Takeuchi, H. Ikuta, D. E. Moncton, and Y. S. Lee, arXiv:1202.4994.